

Proteomic Analysis of Formalin-fixed Prostate Cancer Tissue*[§]

Brian L. Hood‡, Marlene M. Darfler§, Thomas G. Guiel§, Bungo Furusato¶, David A. Lucas‡, Bradley R. Ringeisen||, Isabell A. Sesterhenn¶, Thomas P. Conrads‡, Timothy D. Veenstra‡**, and David B. Krizman‡ ††

Proteomic analysis of formalin-fixed paraffin-embedded (FFPE) tissue would enable retrospective biomarker investigations of this vast archive of pathologically characterized clinical samples that exist worldwide. These FFPE tissues are, however, refractory to proteomic investigations utilizing many state of the art methodologies largely due to the high level of covalently cross-linked proteins arising from formalin fixation. A novel tissue microdissection technique has been developed and combined with a method to extract soluble peptides directly from FFPE tissue for mass spectral analysis of prostate cancer (PCa) and benign prostate hyperplasia (BPH). Hundreds of proteins from PCa and BPH tissue were identified, including several known PCa markers such as prostate-specific antigen, prostatic acid phosphatase, and macrophage inhibitory cytokine-1. Quantitative proteomic profiling utilizing stable isotope labeling confirmed similar expression levels of prostate-specific antigen and prostatic acid phosphatase in BPH and PCa cells, whereas the expression of macrophage inhibitory cytokine-1 was found to be greater in PCa as compared with BPH cells. *Molecular & Cellular Proteomics* 4:1741–1753, 2005.

The ability to correlate results of biomarker discovery investigations to defined disease states promises to improve early detection and provide for targeted therapeutics and markers of drug toxicity. Large scale gene profiling investigations have led to vast amounts of gene expression information on candidate biomarkers, which have proven useful to the understanding of biological and disease processes (1–4). Despite these advances, there is limited information on the gene products that play vital roles in cellular processes including cancer initiation, progression, and metastasis (5). Consequently, a crucial need exists to develop similar large scale approaches for protein biomarker discovery.

From the ‡Laboratory of Proteomics and Analytical Technologies, SAIC-Frederick, Inc., National Cancer Institute, Frederick, MD 21702; §Expression Pathology Incorporated, Gaithersburg, MD 20877; ¶Armed Forces Institute of Pathology, Department of Genitourinary Pathology, Washington, DC 20306; and ||Naval Research Laboratory, Washington, DC 20375.

Received, April 14, 2005, and in revised form, August 8, 2005

Published, MCP Papers in Press, August 9, 2005, DOI 10.1074/mcp.M500102-MCP200

Tissue-based proteomic studies are inherently attractive for relating protein biomarkers directly to disease. Whereas fresh and/or frozen tissue samples may represent attractive samples from which proteomic biomarker investigations may be conducted, they are often difficult to obtain in large numbers and relatively expensive to store in a stable form. Formalin fixation and paraffin embedding of tissue is the standard processing methodology practiced in pathology laboratories worldwide, resulting in a highly stable form of tissue that is easily stored due to its inherent stability at room temperature. Hence, formalin-fixed paraffin-embedded (FFPE)¹ tissues represent a potentially attractive resource for conducting retrospective protein biomarker investigation. Arising from the high degree of covalently cross-linked proteins in FFPE tissue, immunohistochemistry (IHC) is currently the only published technology capable of providing “proteomic” information from these samples, and unfortunately IHC methods lack sensitivity, quantitation, and scalability. Methodologies designed to increase IHC sensitivity by decreasing the effects of formalin-induced protein cross-linking have shown some success, yet quantitation and scalability issues remain (6, 7). In addition, IHC requires *a priori* knowledge of individual proteins being analyzed, thereby limiting biomarker discovery approaches. Other methods to procure and assay soluble proteins directly from FFPE tissue have also shown limited success on a small scale (8–10). Development of the capability to conduct large scale analyses of tissues using proteomics approaches analogous to the scale and throughput of high throughput gene expression analysis could have far reaching implications on protein biomarker investigations of disease through interrogation of the vast archived FFPE tissue collections.

Laser-based tissue microdissection has enabled molecular analysis of specifically defined populations of cells captured directly from their tissue microenvironment (3, 11–13). Despite recent interest in conducting tissue microdissection of FFPE

¹ The abbreviations used are: FFPE, formalin-fixed paraffin-embedded; IHC, immunohistochemistry; LT, Liquid Tissue™; nanoRPLC, nanoflow reversed-phase liquid chromatography; BPH, prostate hyperplasia; CCD, charge-coupled device; PCa, prostate cancer; PSA, prostate-specific antigen; CAD/CAM, computer-aided design/computer-aided machining; OCT, optimal cutting temperature compound; LIT, linear ion trap.

tissues for mRNA extraction and analysis, microdissection of FFPE tissues is not widely practiced due to lack of technological optimization for fixed tissue and lack of methodologies for extraction and analysis of soluble protein (14–17).

Dramatic improvements in MS instrumentation and the rapid growth of genomic databases have enabled development of high throughput proteomic approaches to identify and quantify large numbers of proteins from complex samples such as cancer cell lysates (5, 18–21). Identification of proteins by MS in cells obtained by microdissection of fresh frozen tissue has recently been demonstrated (22, 23). The combined application of tissue microdissection and MS analysis of FFPE tissue has the potential for generating protein biomarker data necessary for dissecting those elements key to the pathological manifestation of cancer and other diseases.

We have utilized a novel tissue microdissection technique optimized for the extraction of cells from FFPE tissue and a biochemical methodology for the recovery of soluble proteins and peptides suitable for analysis by nanoflow reversed-phase liquid chromatography (nanoRPLC)-MS/MS for a proteomic investigation of benign prostate hyperplasia (BPH) and prostate cancer (PCa) tissue. The data presented demonstrate the potential for identification of proteins and their relative expression levels and relate this information to a particular disease state from FFPE tissue. This study represents the first differential large scale proteome analysis from FFPE-archived tissue. Furthermore, this study provides a technological framework by which the vast archive of pathologically characterized FFPE clinical samples may be analyzed utilizing state of the art MS-based proteomic technologies.

MATERIALS AND METHODS

Materials—Formic acid (HCOOH), TFA, and DTT were purchased from Sigma. Porcine sequencing grade modified trypsin was obtained from Promega. HPLC-grade ACN (CH₃CN) was obtained from EMD Chemicals Inc. (Gibbstown, NJ). All buffers and reagents were used as supplied from the manufacturer and prepared in double-distilled water using a NANOPure Diamond water system (Barnstead International, Dubuque, IA). The Liquid Tissue-ID (LT-ID) protein prep kit and the Liquid Tissue-MS (LT-MS) protein prep kit were obtained from Expression Pathology, Inc. (Gaithersburg, MD).

Tissue Pathology and Processing—A FFPE whole-mount prostate case was chosen and histologically analyzed by standard methods. 5- μ m-thick sections were cut and placed on glass slides and stained with hematoxylin and eosin for identification of histologically distinct tissue regions. Histological analysis was performed on an Olympus BX51 microscope, and images (10 \times 20 magnification) were taken with an Olympus Q color camera mounted on the microscope. The IHC analysis for prostate-specific antigen (PSA) was performed using standard methodologies with a mouse monoclonal anti-PSA primary antibody (Dako Cytomation, Carpinteria, CA) and standard colorimetric detection methods.

For tissue microdissection, 10- μ m-thick tissue sections were cut from the FFPE whole-mount prostate tissue block, placed on the coated slides, and heated for 60 min at 58 $^{\circ}$ C. Paraffin was removed by treatment in SubX organic solvent (Surgipath Medical Industries, Richmond, IL) twice for 5 min; this was followed by tissue rehydration

through multiple, graded ethanol solutions and distilled water. Tissue was counterstained with Mayer's hematoxylin, dehydrated through graded ethanol solutions, and air-dried. Tissue was rehydrated prior to microdissection with 50% glycerol in water for 5 min. Slides were placed upside down below the 10 \times objective and visualized to locate cellular regions with specific histological features, which were mapped using the accompanying stage software. The microdissection was automated, allowing for modulation of the laser and scanning of the receiving substrate via computer-aided design/computer-aided machining (CAD/CAM). Microdissection was performed by software directed laser pulses to strike at a constant velocity and rate throughput over the previously defined and mapped cellular regions to achieve complete transfer of cells within the selected area into a 1.5-ml low binding microcentrifuge receiving tube.

The tissue microdissection instrument is based on an optical setup designed to direct a pulsed laser onto a target slide holding a 10- μ m-thick tissue section. An excimer laser (MPB Technologies PSX-100) operating at the following conditions was utilized for microdissection: 248 nm wavelength, 2.5 ns pulse, E_{\max} = 5 mJ, repetition rate = 0.1–100 Hz. Target slides are made of optically transparent quartz with an energy transfer coating with the exact dimensions of a standard histology glass slide. The slide stage is a computer controlled, XY translation stage with a maximum translation speed of 200 mm/s. The laser is split by a 1/8 beam splitter to an energy meter, and the remaining beam travels to an UV reflective mirror and directed down ($-Z$) to a 10 \times microscope objective (LMU-10 \times -UVR, OFR), which focuses the laser onto the slide and allows for observation of the dissection process via a confocally aligned CCD camera.

To assess the impact of formalin fixation on the ability to identify peptides extracted from FFPE tissue sections, a liver was procured from a freshly sacrificed male C57 black mouse. A lobe of the liver was cut into two equal sections. One section of the liver was frozen on dry ice and placed at -80° C prior to embedding in optimal cutting temperature compound (OCT) and cryosectioned. The other section was immediately placed in 10% buffered formalin for 96 h prior to embedding in paraffin and sectioning. The frozen tissue sections were placed in 70% ethanol for 30 s and then distilled water for 30 s to remove the OCT, followed by dehydration in 70, 85, and 100% ethanol and quickly air dried. The FFPE liver tissue was deparaffinized in two changes of SubX for 5 min followed by rehydration through graded ethanol solutions and distilled water. The entire sections from both the formalin-fixed and frozen tissues were placed separately in 20 μ l of LT-MS buffer, processed, and analyzed by nanoRPLC-MS/MS as described below.

Protein Extraction—Cells collected by microdissection for array analysis and nanoRPLC-MS/MS analysis were processed by reagents according to the manufacturer's recommendations (Expression Pathology, Inc.). Cellular material for array analysis was suspended in 20 μ l of LT-ID buffer A, incubated at 95 $^{\circ}$ C for 90 min, then cooled on ice for 3 min at which time 1 μ l of LT-ID buffer B was added followed by incubation at 37 $^{\circ}$ C for 1 h. Samples were stored at -20° C until analysis. Cellular material for nanoRPLC-MS/MS analysis was suspended in 20 μ l of LT-MS reaction buffer, incubated at 95 $^{\circ}$ C for 90 min, then cooled on ice for 3 min at which time 1 μ l of trypsin (15–18 U) was added followed by incubation at 37 $^{\circ}$ C overnight. DTT was added to a final concentration of 10 mM, and the samples were heated for 5 min at 95 $^{\circ}$ C to reduce cysteine residues. Digestates were stored at -20° C until analysis.

Protein Microarray Assay—Two-fold serial dilutions of protein extracts were arrayed in duplicate on a nitrocellulose membrane using a manual arrayer (V&P Scientific, Inc., San Diego, CA). A protein dot blot assay for PSA expression was performed using standard immunoassay conditions with a mouse monoclonal anti-PSA primary antibody (DakoCytomation) and a biotinylated anti-mouse IgG secondary an-

tibody (Pierce Biotechnology, Inc.), streptavidin-alkaline phosphatase (Pierce Biotechnology, Inc.), and nitroblue tetrazolium/5-bromo-4-chloro-3-indolyl phosphate substrate (Moss, Inc., Pasadena, MD) for colorimetric signal detection. Images of the membrane were captured by a CCD camera as a TIFF file and analyzed with image analysis software (GridGrinder, Corning Incorporated, Corning, NY) for spot intensity. The data were imported into a Microsoft Excel for graphing and statistical analysis.

Sample Preparation and Trypsin-mediated ^{18}O Labeling—Tryptic peptides generated from BPH and PCa cells were desalted using C-18 ZipTip microcolumns (Millipore, Billerica, MA), lyophilized to dryness, and resuspended in 0.1% TFA for nanoRPLC-MS/MS analysis. For the isotope labeling, protein extracts from an approximately equivalent number of microdissected cells were lyophilized and reconstituted separately in H_2^{16}O (BPH) and H_2^{18}O (PCa) each containing 20% methanol (v/v). Porcine sequencing grade trypsin (Promega) was resuspended in the appropriately labeled water and added to each sample at an enzyme-to-protein ratio of 1:20. Samples were incubated for 16 h at 37 °C, after which an additional equivalent aliquot of the trypsin solution was added, and the samples were incubated for an additional 6 h. Because tryptic peptides are produced via the extraction of the proteins from the cells dissected from the FFPE tissues, the role of trypsin during this step is to enzymatically exchange the C-terminal carboxyl oxygen atoms with the appropriate isotope. TFA was added to a final concentration of 0.4% (v/v), and the solutions were boiled for 10 min. Samples were pooled, lyophilized to dryness, and resuspended in 0.1% TFA prior to analysis.

NanoRPLC-MS/MS Analysis—NanoRPLC was performed using an Agilent 1100 capillary LC system (Agilent Technologies, Palo Alto, CA) coupled on-line to either a linear ion trap (LIT) mass spectrometer (LTQ, Thermo Electron, San Jose, CA) or a hybrid LIT-FT-ICR MS. NanoRPLC separations of each sample were performed using 75- μm inner diameter \times 360 outer diameter \times 10-cm-long fused silica capillary columns (Polymicro Technologies, Phoenix, AZ) that were slurry packed in-house with 3 μm , 300 Å pore size C-18 silica bonded stationary phase (Vydac, Hysperia, CA). After injecting 1 μl of sample, the column was washed for 30 min with 98% mobile-phase A (0.1% formic acid in water) at a flow rate of 0.5 $\mu\text{l}/\text{min}$. Peptides were eluted using a linear gradient of 2% mobile-phase B (0.1% formic acid in ACN) to 40% solvent B in 110 min, then to 98% B in an additional 30 min, all at a constant flow rate of 0.25 $\mu\text{l}/\text{min}$.

The LIT-MS was operated in a data-dependent MS/MS mode in which each full MS scan is followed by five MS/MS scans where the five most abundant peptide molecular ions are selected for CID using a normalized collision energy of 35%. Dynamic exclusion was utilized to minimize redundant selection of peptides previously selected for CID. The heated capillary temperature and electrospray voltage were set at 160 °C and 1.5 kV, respectively. Data were collected over a broad mass to charge (m/z) precursor ion selection scan range of 400–2000 followed by eight segmented precursor selection scan ranges (e.g. gas phase fractionation in the m/z dimension, GPF _{m/z}) using the following overlapping m/z intervals: m/z 400–605, 595–805, 795–1005, 995–1205, 1195–1405, 1395–1605, 1595–1805, 1795–2000, 400–805, and 795–1200. Data for the $^{16}\text{O}/^{18}\text{O}$ -labeled BPH/PCa experiment was acquired using FT-ICR detection in centroid mode for the full MS scan (m/z 200–2000) at 100,000 resolution followed by MS/MS using the LIT on the top five molecular ions detected in the FT-ICR scan.

Bioinformatic Analysis—Tandem mass spectra were searched against the UniProt human and mouse proteomic databases (01/04/05 release) from the European Bioinformatics Institute (www.ebi.ac.uk/integr8) using SEQUEST (Thermo Electron). Peptides were searched using fully tryptic cleavage constraints and a dynamic

4.008-amu modification on the C terminus for the ^{18}O isotope-labeling analysis. For a peptide to be considered legitimately identified, it had to achieve stringent charge state and proteolytic cleavage-dependent cross-correlation (X_{corr}) scores of 1.9 for $[\text{M}+\text{H}]^{1+}$, 2.2 for $[\text{M}+2\text{H}]^{2+}$, and 3.5 for $[\text{M}+3\text{H}]^{3+}$ (3.1 for the ^{18}O -labeling analysis), and a minimum delta correlation score (ΔC_n) of 0.08. SEQUEST results were further filtered using software developed in-house to determine unique peptides and proteins. To evaluate false positive identifications, the entire PCa dataset was searched against a reversed human protein database in a similar fashion as previously described (24). The calculations reveal that using the SEQUEST parameters described above results in less than 1.5% of the identifications in each dataset being classified as a false positive.

The molecular function and cellular localization of the unique proteins identified in the various analyses performed in this study were categorized by gene ontology (www.geneontology.org). GRAVY values for each unique protein were calculated according to the method of Kyte and Doolittle (25).

RESULTS

Tissue Pathology and IHC Analysis—A whole-mount FFPE prostate tissue block procured from a radical prostatectomy was utilized for this study. This tissue displayed a range of well, moderate, and poorly differentiated carcinoma of intermediate grade, prostatic intraepithelial neoplasia, and glandular hyperplasia. Histological analysis of this whole-mount prostate (Fig. 1A) indicates prostatic carcinoma, well, moderately, and poorly (5%) differentiated, nuclear grade II (Gleason 3 + 4); carcinoma, well and moderately differentiated, nuclear grade II (Gleason 3 + 3); carcinoma, well and moderately differentiated, nuclear grade I (Gleason 3 + 3) (PCa 2 region); carcinoma, well and moderately differentiated, nuclear grade I (Gleason 3 + 3) (PCa 1 region); two microscopic foci of carcinoma, well differentiated, nuclear grade I; prostatic intraepithelial neoplasia; glandular hyperplasia (BPH 1 and 2 regions); pathological stage pT (6)2cNxMx; surgical margin negative.

To demonstrate the ability to extract soluble, dilutable, immunoreactive protein from FFPE tissue, IHC was employed to identify tissue regions that express PSA. Standard hematoxylin and eosin-stained whole-mount tissue sections from the prostate tissue block show two tumor regions (indicated PCa 1 and PCa 2), two BPH regions (BPH1 and BPH2), and a stromal region (Fig. 1A). The IHC analysis revealed that epithelial cells and most regions over the entire tissue section stained positive (brown color) for PSA expression (PSA+), including the tumor epithelial regions PCa 1 and 2, and both BPH epithelial components (BPH 1 and 2), while the stromal regions stained negative (PSA-) (Fig. 1B).

Tissue Microdissection—10- μm -thick prostate tissue sections were cut and placed on single energy transfer-coated slides for microdissection. Approximately 200,000 cells from each of the two PSA+ tumor regions (PCa 1 and 2), 200,000 cells from each of the two PSA+ BPH regions (BPH 1 and 2), and 100,000 cells from the PSA- stromal region were microdissected (Fig. 1C) using a novel tissue microdissection technique developed specifically for FFPE tissue, termed the *Ex-Cellerator*TM. The energy transfer layer between the slide and

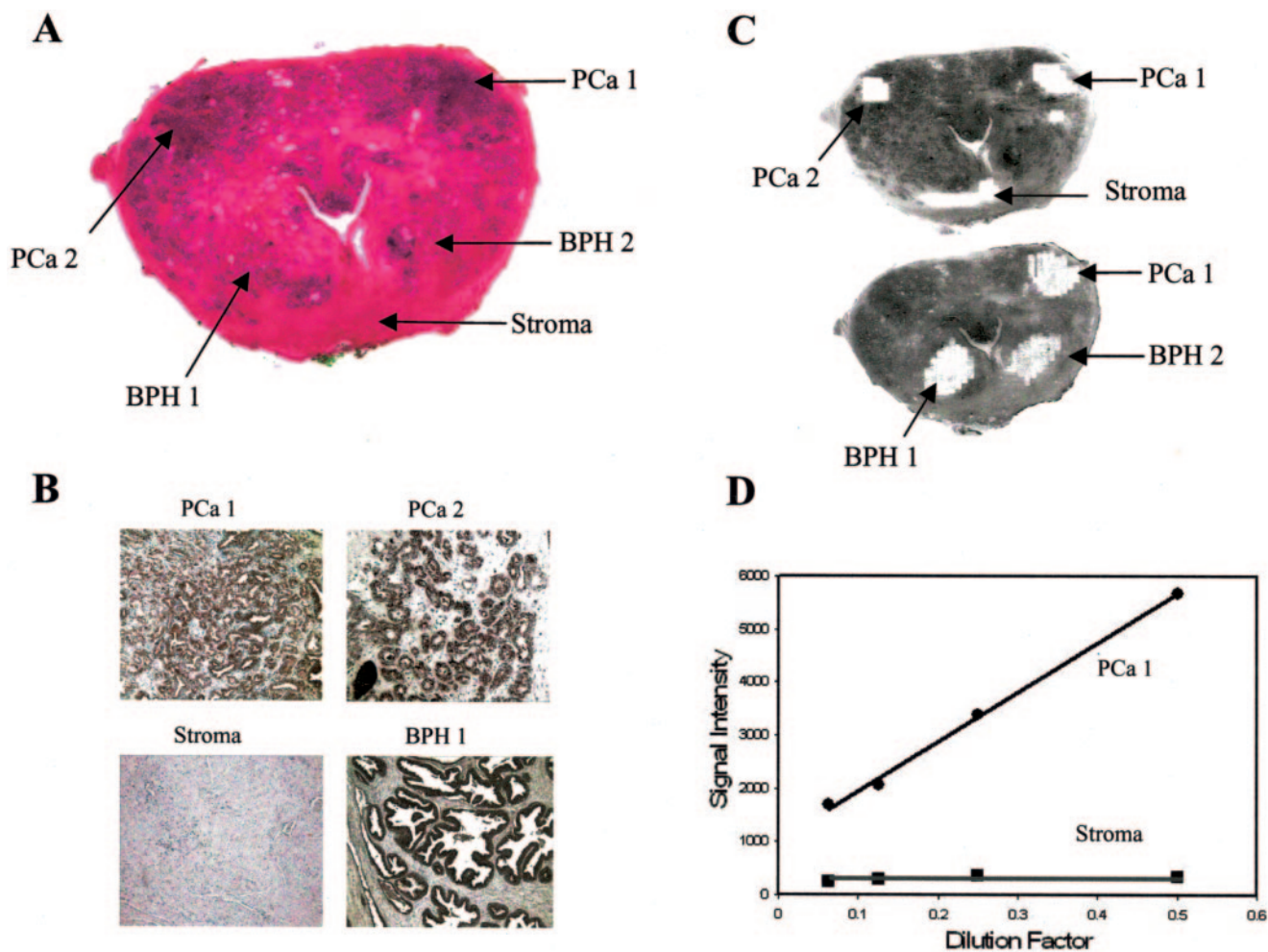


FIG. 1. Immunohistochemistry, microdissection, and protein assay of FFPE prostate tissue. *A*, standard hematoxylin and eosin analysis identified multiple histological lesions within a whole-mount prostate tissue section. Two large regions of Gleason grade 3 tumor (PCa 1 and PCa 2), a single large region of stroma, and two large regions of BPH (1 and 2) were identified for tissue microdissection. *B*, IHC analysis of PSA. A single whole-mount section from the tissue block was analyzed for expression of PSA by standard IHC. The epithelial component of regions PCa 1, PCa 2, BPH 1, and BPH 2 are positive for PSA expression, whereas stromal components in each of these regions and the stromal region are negative for PSA. *C*, post-microdissection tissue of identified regions of PCa (1 and 2), BPH (1 and 2), and stroma. *D*, cells were microdissected from regions PCa 1 and stroma separately, and protein extracts were prepared. Protein was diluted in 2-fold serial dilutions and arrayed in duplicate on nitrocellulose membranes followed by a standard colorimetric immunodetection method with a monoclonal anti-PSA antibody. Dot blot results of spot signal intensity versus protein dilution factor graphically demonstrate solubility/dilutability of the protein extracts, positive expression of PSA in PCa 1 region, and lack of PSA expression in the stromal region.

tissue section imparts a photoabsorption process where each incident laser pulse removes a three-dimensional pixel of tissue from the quartz slide, propelling it into a receiving tube. The amount of tissue transferred in a single pixel is a function of the diameter of the laser, the tissue thickness, and the laser fluence. The software controlling the moveable stage that held the tissue slide was programmed to perform CAD/CAM microdissection of specific demarcated cellular regions for microdissection. Laser repetition rates were at a constant 99 Hz, allowing for transfer of all cells in a marked region within seconds. A CCD camera positioned in line with the optical setup allowed for tissue visualization, identification of cell populations for microdissecting, and real-time analysis/mon-

itoring of the transfer process. The total number of microdissected cells was approximated by determining the area of the lesion marked for CAD/CAM-controlled microdissection, the approximate diameter of a single cancer cell (15 μm), and thickness of the section (10 μm).

Protein Microarray Analysis—Protein extracts were prepared for microarray analysis from the tumor epithelial PCa 1 and stromal regions, serially diluted, and spotted on a microarray in duplicate along with buffer. Approximately 90 cell equivalents of protein were spotted at the high end of the 2-fold dilution series. Standard immunoassay detection of the protein array with a monoclonal anti-PSA antibody indicates positive detection of PSA in the sample prepared from the

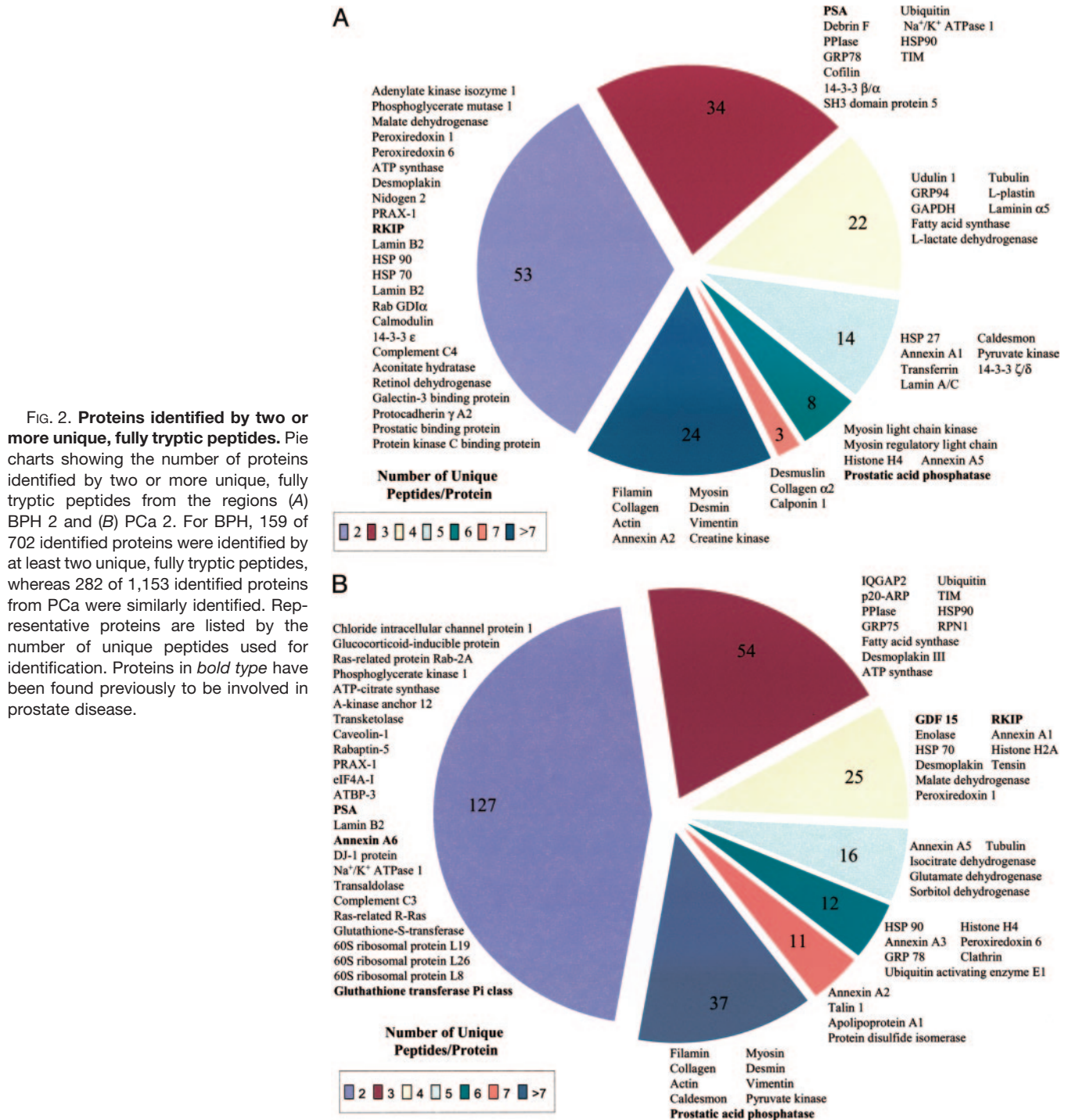


FIG. 2. **Proteins identified by two or more unique, fully tryptic peptides.** Pie charts showing the number of proteins identified by two or more unique, fully tryptic peptides from the regions (A) BPH 2 and (B) PCa 2. For BPH, 159 of 702 identified proteins were identified by at least two unique, fully tryptic peptides, whereas 282 of 1,153 identified proteins from PCa were similarly identified. Representative proteins are listed by the number of unique peptides used for identification. Proteins in *bold type* have been found previously to be involved in prostate disease.

PSA+ epithelial cancer area (PCa 1), whereas no PSA was detected in the sample prepared from the PSA- stromal area (results shown graphically in Fig. 1D). This indicates the ability to detect PSA expression in a microarray format and demonstrates the dilutability of extracted protein from formalin-fixed tissue. A duplicate parallel array assayed without primary PSA antibody showed no signal (data not shown). All samples were normalized for protein concentration.

Analysis of Peptides by MS—To investigate the potential utility of conventional MS-based proteomic methods for conducting identification of peptides extracted from FFPE PCa tissue, ~200,000 cells from PCa 2 and BPH 2 regions (Fig. 1, A and C) were microdissected as described and analyzed by nanoRPLC-MS/MS. Approximately 100,000 cell equivalents of protein from each extract were analyzed by nanoRPLC-MS/MS, resulting in the identification of over 1,300 and 2,200

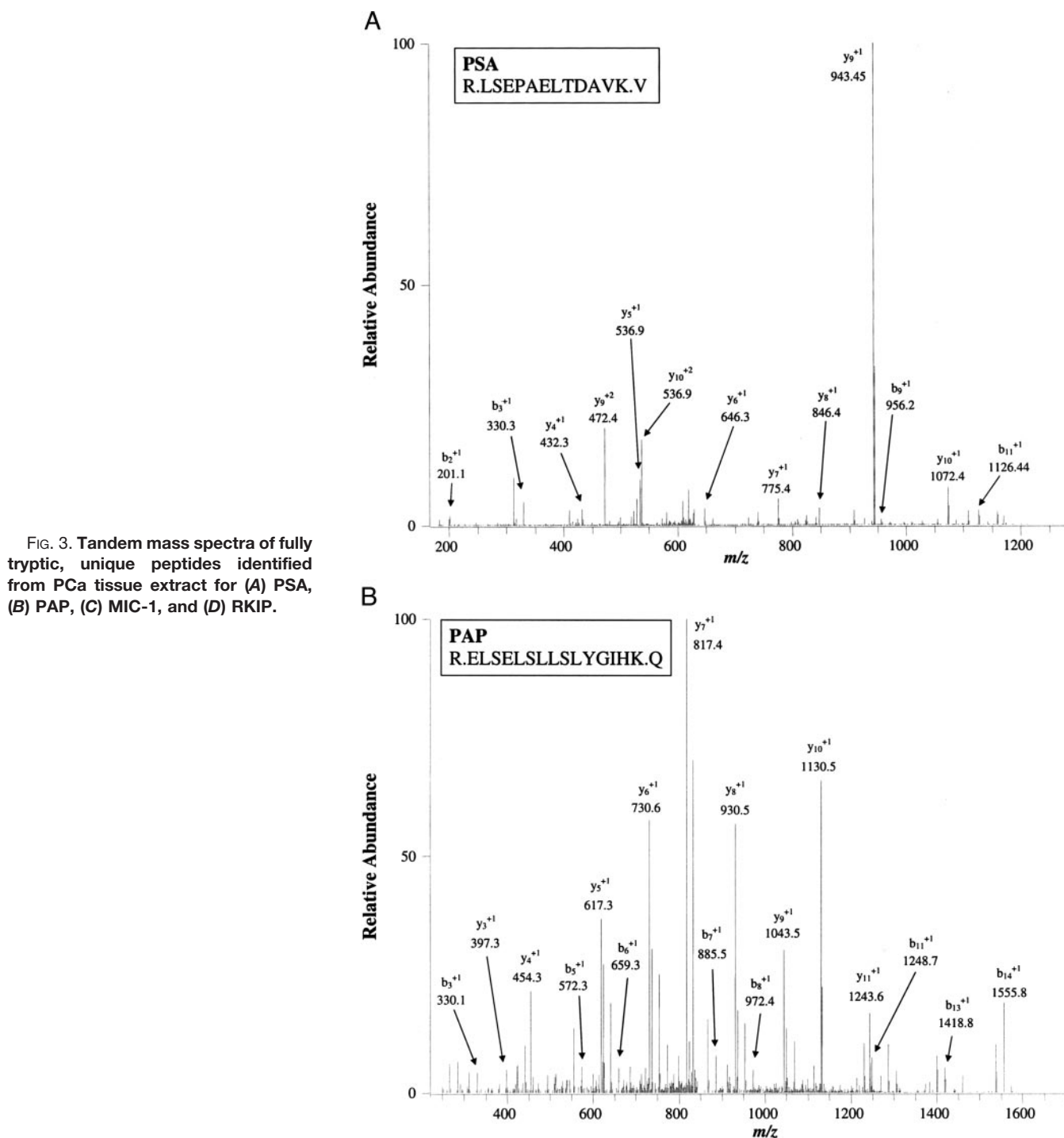


FIG. 3. Tandem mass spectra of fully tryptic, unique peptides identified from PCa tissue extract for (A) PSA, (B) PAP, (C) MIC-1, and (D) RKIP.

unique, fully tryptic peptides representing 702 and 1,156 unique proteins, from the BPH and PCa FFPE tissue extracts, respectively (supplemental Tables 1 and 2). Of these proteins, roughly 25% were identified by two or more unique peptides in both tissue extracts (Fig. 2, A and B).

As anticipated, many of the proteins identified by the greatest number of unique peptides represent highly abundant cytoskeletal proteins (*i.e.* actin, collagen, myosin, etc.). A va-

riety of prostate-related proteins were identified in this investigation as expressed in microdissected PCa tissue extract including PSA, prostatic acid phosphatase (PAP), macrophage inhibitory cytokine-1 (MIC-1), and Raf kinase inhibitor protein (RKIP) (Fig. 3, A–D). Many of these markers were identified by multiple unique peptides in the protein extracts obtained from both PCa and BPH cells. PAP was identified by eight and six unique peptides in the protein extracts obtained

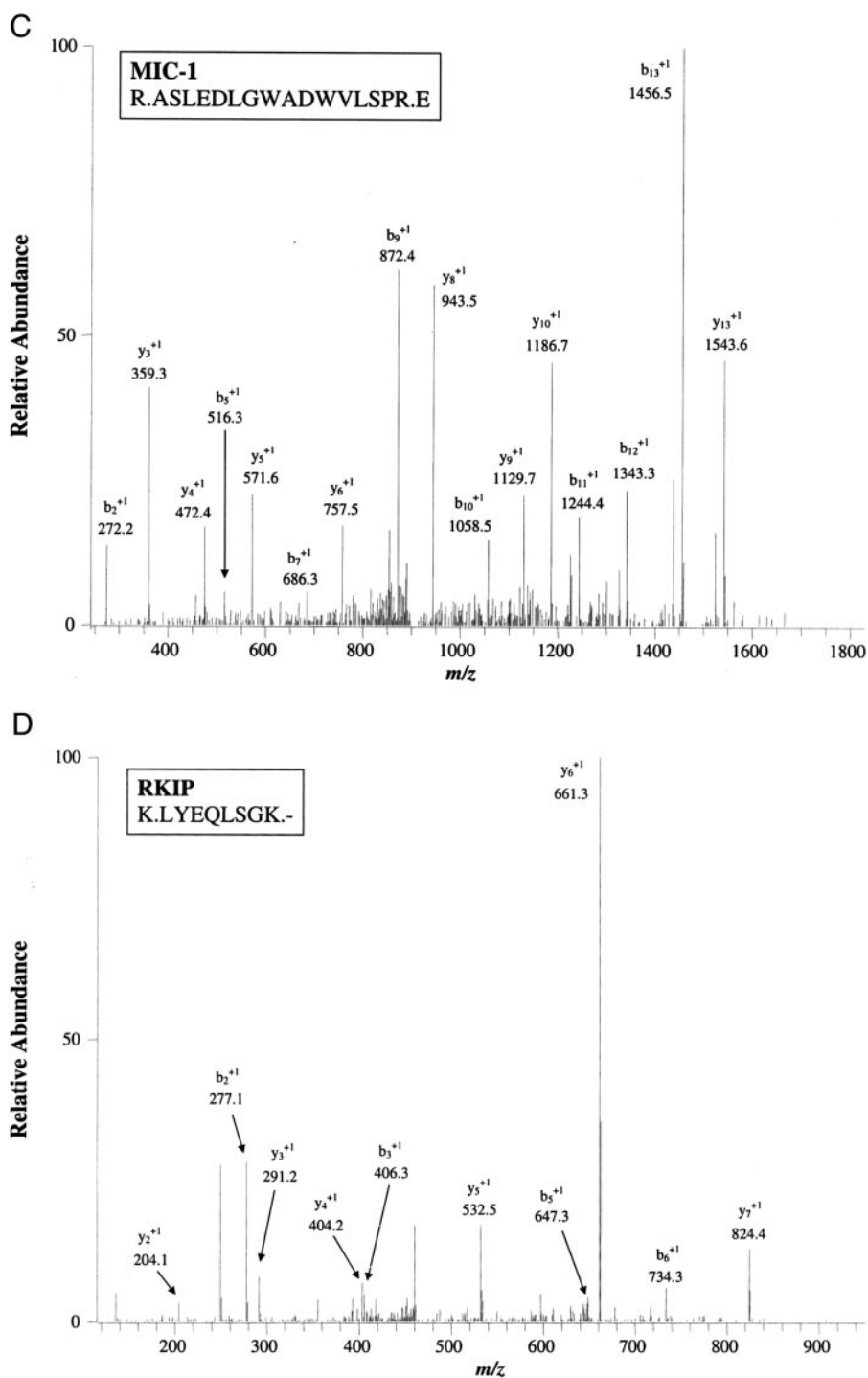


FIG. 3—continued

from the PCa and BPH cells, respectively, whereas PSA was identified by two unique peptides from the PCa microdissection and three unique peptides from the BPH. In contrast, growth differentiation factor 15, otherwise known as MIC-1, was identified by four unique peptides in the protein extracted from the PCa cells, whereas no peptides corresponding to MIC-1 were identified in the protein extracted from the BPH cells.

An obvious concern when examining peptides extracted

from FFPE tissues is the possibility of covalent modifications resulting from formalin fixation and long-term storage. To examine for possible modifications resulting from formalin fixation, a subset of the nanoRPLC-MS/MS analyses of the FFPE PCa cells were searched for lysyl formylation, a likely occurrence arising from formalin fixation. The results indicate that ~6.5% of the identified peptides contain formylated lysyl residues. Unfortunately, the chemistry of formalin fixation and

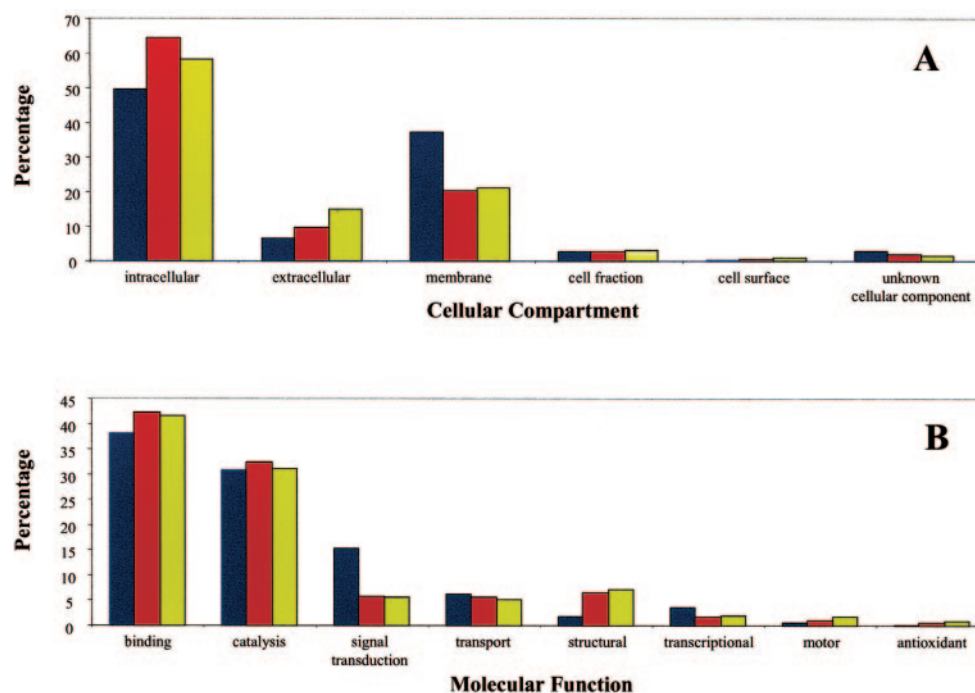


FIG. 4. Gene ontology classification comparing the cellular compartment and molecular function of the identified proteins extracted from FFPE PCa (red) and BPH tissue (yellow). The cellular compartment and molecular functions of all of the classified proteins within the human proteome is also shown (blue).

is still not well understood; therefore a complete investigation of the possible peptide modifications remains to be performed. An examination of the effect of long-term storage showed that 53.1% of the methionine residues within the peptides identified in the analysis of this PCa subset were oxidized. In a previously published global analysis of yeast tryptic peptides that claims a false positive rate of less than 1%, 63% of methionine residues within identified peptides were found to be oxidized (24). The results suggest that formalin fixation and storage do not result in an inordinate degree of oxidation. The results of this study cannot completely address the effects of formalin fixation or long-term storage on tissue samples. As such, any biological conclusions presented in this study are based solely on the identification and quantitation of strictly unmodified peptides.

To determine if formalin fixation impacts trypsin enzymatic specificity, the numbers of peptides identified from the PCa tissue analysis with arginyl and lysyl termini were tabulated. The results show that the percentage of peptides identified with arginyl or lysyl termini is 56 and 44%, respectively. Considering that the prevalence of these two residues within proteins is roughly equivalent (*i.e.* 5.7% of all residues) the most probable outcome would have been a 50:50 distribution of peptides identified containing arginyl and lysyl termini. Although the present results do not exactly match the theoretically predicted distribution, they do not differ significantly enough to draw a reasonable conclusion, suggesting that formalin fixation does not have a negative impact on the enzyme specificity of trypsin.

The number of identified peptides that contain internal missed tryptic cleavage sites was also evaluated. Approximately 25% of the identified peptides contain an internal missed cleavage site. Although this percentage is at the high end, this result may be caused by the fact that certain regions of the proteins may not be completely unfolded or denatured, and therefore some arginyl and lysyl residues are not fully accessible to trypsin.

The molecular functions and cellular localization of the proteins identified in the analysis of the FFPE PCa and BPH tissue samples were classified using gene ontology as shown in Fig. 4. The identified proteins were found to have a broad range of molecular functions and arose from every cell compartment. The gene ontology classification of the proteins identified in these two samples was compared with the proteins within the entire human protein database. This analysis demonstrates that there is no significant bias in the spectrum of proteins identifiable from FFPE tissues. Whereas the human proteome database is predicted to contain a higher percentage of membrane proteins than observed in the present result from the proteomic analysis of FFPE PCa and BPH tissue, this observation is not surprising considering the present sample preparation methodology lacks any specific protocol for membrane protein enrichment. In the case of signal transduction proteins, the analysis of the FFPE tissues revealed a lower percentage than that classified within the human proteome. It is important to point out, however, that signal transduction proteins are considered to be low abun-

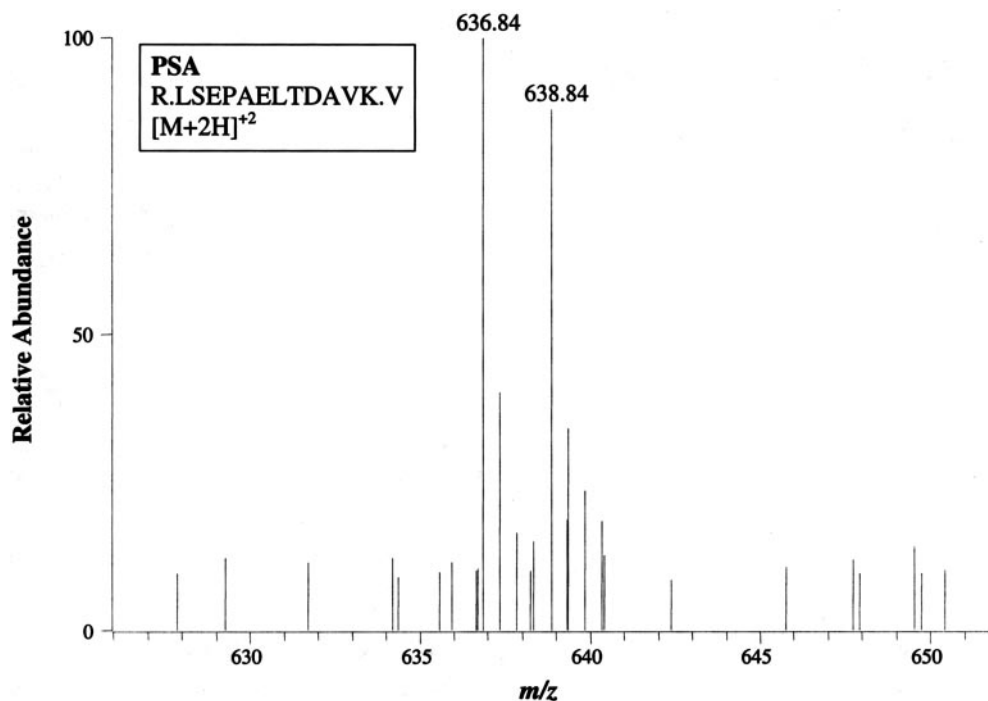


FIG. 5. Mass spectrum of the $^{16}\text{O}/^{18}\text{O}$ molecular ion pair of a PSA peptide from the isotope-labeling experiment showing a 2-Da mass shift for the $[\text{M}+2\text{H}]^{+2}$ molecular ion with an isotomeric ratio of ~ 1.0 .

dant proteins, and therefore it would be expected that they would be somewhat underrepresented in this analysis compared with their preponderance in the human proteome. The range of hydrophobicity values for the proteins identified from the PCa and BPH tissues was also calculated (25). The proteins identified in each set show similar results and covered the complete range of GRAVY values (*i.e.* -2.5 to $+2.5$). A majority of the proteins are slightly hydrophilic in nature (calculated hydrophobicity values of 0 to -1), slightly lower than that observed for the entire human protein database (data not shown). In general, these results are consistent with other global proteomic analyses performed in our laboratory (26, 27).² A comparison of the data shows that a global proteome analysis of FFPE tissue samples utilizing the described methodology results in a broad coverage of protein localization and function.

In addition to the “subtractive proteomics” approach to determine differential and total unique peptide identifications as described previously, trypsin-mediated ^{18}O isotope labeling was utilized to ascertain differential protein expression between microdissected BPH and PCa tissue extracts. Trypsin digestates from a total of 200,000 microdissected cells (Fig. 1, A and C) from each pathologically distinct prostate tissue region (BPH 1 and PCa 1) were prepared and lyophilized. The BPH extract was resuspended in a buffered solution

prepared in H_2^{16}O , and the PCa extract was resuspended in the identical buffered solution prepared in H_2^{18}O . The addition of trypsin to these samples mediates the exchange of two equivalents of ^{16}O at the carboxyl terminus of each peptide for two equivalents of ^{18}O in the sample reconstituted in H_2^{18}O . Two complete enzyme turnovers in the presence of H_2^{18}O results in approximately a 4-Da increase in mass of each tryptic peptide compared with those peptides maintained in H_2^{16}O (28–30). Many of the same proteins identified in the global analysis were identified in the isotope-labeled samples, including PSA, PAP, and other prostate disease-related proteins (supplemental Table 3). Indeed, PSA was identified with approximately equivalent abundance levels in each tissue region based on the $^{16}\text{O}/^{18}\text{O}$ isotope ratio (Fig. 5), whereas only a single ^{18}O -containing (*i.e.* from PCa cells) MIC-1 peptide was observed.

An analysis comparing the number of peptides/proteins that can be identified from an equivalent number of fresh frozen and FFPE cells was performed to determine the effect of formalin cross-linking and paraffin embedding on peptide extraction efficiency. Mouse liver tissue was cut into two equivalently sized sections where one of the sections was frozen and embedded in OCT while the other was formalin-fixed and paraffin-embedded. A tissue slice was cut from the face of each sample, and $\sim 30,000$ cells were extracted from each and processed using the described methodology. Representative base peak chromatograms of the nanoRPLC-MS/MS analysis of the peptides extracted from the FFPE and frozen liver sections are shown in Fig. 6, A and B, respectively,

² B. L. Hood, M. M. Darfler, T. G. Guiel, B. Furusato, D. A. Lucas, B. R. Ringeisen, I. A. Sesterhenn, T. P. Conrads, T. D. Veenstra, and D. B. Krizman, unpublished data.

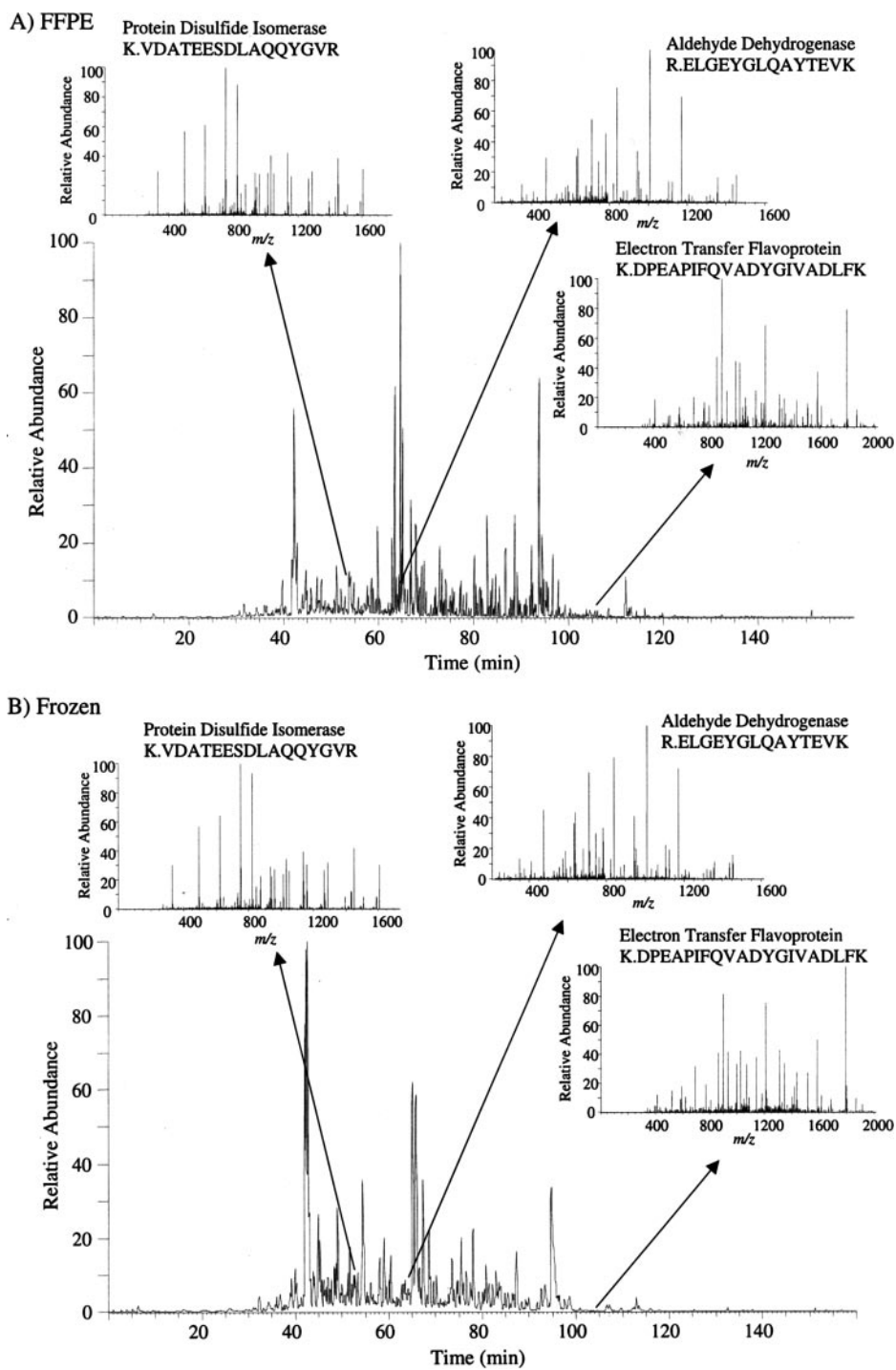


FIG. 6. Comparison of base peak chromatograms and selected MS/MS spectra of peptides extracted from (A) FFPE and (B) frozen liver tissue sections.

revealing similar base peak chromatograms profiles. A comparison of three selected MS/MS spectra is also shown in Fig. 6, A and B. These spectra illustrate the similarity in the MS/MS spectra with respect to peptide CID as well as elution time. From this analysis, 2,001 unique peptides corresponding to 776 unique proteins were identified from the frozen tissue section, whereas 1,710 unique peptides corresponding to 684 unique proteins were identified from the FFPE liver tissue

(Table I). A gene ontology classification of the identified proteins shows similar protein functions and localizations in both tissues (Fig. 7). A comparison of the top 15 proteins identified on the basis of sequence coverage from the FFPE tissue with the same proteins identified from the frozen liver tissue demonstrates excellent correspondence (Table II). For example, in both samples a protein that is weakly homologous to human carbamoyl phosphate synthase was by far the most identified

FIG. 7. Gene ontology classification comparing the cellular compartment and molecular function of the identified proteins extracted from FFPE (blue) and fresh frozen (yellow) liver tissue.

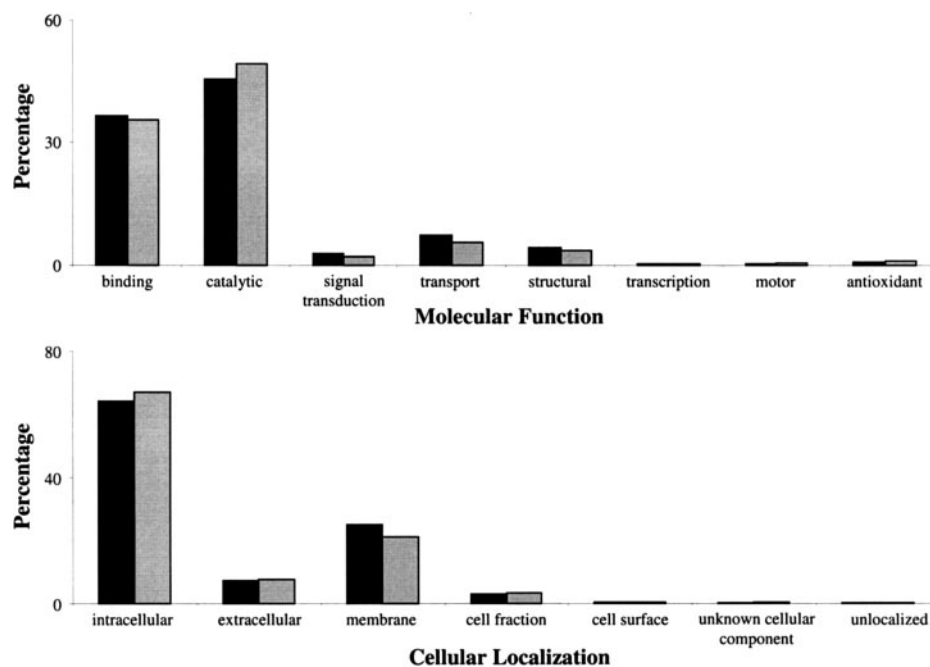


TABLE I
Comparison of the number of unique peptides and proteins identified from FFPE and frozen liver tissue

Sample	No. of unique peptides	No. of unique proteins
FFPE tissue	1,710	684
Frozen tissue	2,001	776

protein with 72 and 91 unique peptides identified from the FFPE and frozen tissue, respectively. This demonstrates that despite the potentially negative impact imparted from the FFPE process on the efficient extraction of proteins, a significant (and nearly similar) amount of proteomic information can be extracted from these samples as compared with fresh, frozen tissue samples.

DISCUSSION

A MS-based proteome analysis of FFPE prostate tissue has been conducted resulting in the identification of thousands of unique proteins in various histological regions of the tissue sample. The results presented demonstrate the ability of a protein solubilization methodology to enable global proteomic investigations of microdissected FFPE cancerous tissue. A variety of prostate-related proteins were identified in this investigation as expressed in microdissected PCa tissue extract including PSA, PAP, MIC-1, and RKIP (Fig. 3, A–D). PAP, which is believed to be involved in benign and malignant prostate epithelial cell growth (31), has previously been used as a diagnostic marker for PCa but has low tumor sensitivity and specificity (32, 33). MIC-1 is a member of the transforming growth factor- β superfamily of proteins that play a role in pro- and anti-inflammatory responses to infection (34, 35). It

TABLE II
Comparison of the number of unique peptides identified for the top 15 proteins identified within the FFPE tissues with the number of unique peptides identified for each protein extracted from frozen tissue

Protein	UniProt accession no.	No. of unique peptides	
		FFPE tissue	Frozen tissue
Carbamoyl-phosphate synthase	Q8C196	72	91
78-kDa glucose-regulated protein	P20029	33	21
ATP synthase β chain	P56480	32	34
60-kDa heat shock protein	P63038	32	33
10-formyltetrahydrofolate dehydrogenase	Q8R0Y6	31	41
Catalase	P24270	30	12
Hydroxymethylglutaryl-CoA synthase	P54896	29	23
Acetyl-CoA acyl transferase	Q8BWT1	27	27
GST	P10649	25	21
Pyruvate carboxylase	Q05920	24	21
Argininosuccinate synthase	P16460	23	15
Homocysteine S-methyltransferase	O35490	23	43
Fatty acid-binding protein	P12710	22	3
Triacylglycerol hydrolase	Q8VCT4	22	12
Selenium-binding protein 1	P17563	21	7

has been shown that MIC-1 is highly expressed in PCa tissue and may play a role in the inflammatory process that contributes to PCa susceptibility (36). RKIP, previously identified as phosphatidylethanolamine binding protein, is involved in a variety of signaling pathways and has been observed to have anti-metastatic and pro-apoptotic processes (35, 36). Prior studies have revealed that lower protein levels of RKIP in prostate tissue reduces cellular apoptosis and results in increased tumor metastases (37, 38).

Analysis of the BPH-microdissected tissue extract yielded

similar results with a few notable distinctions. A number of the prostatic markers identified in the cancer extract were identified by similar numbers of unique peptides in the BPH extract. Indeed, PSA was identified by an additional unique peptide in BPH, and IHC revealed the presence of PSA in both cancer and BPH regions from the same tissue section. This is not surprising because PSA has been under significant scrutiny for its inability to accurately distinguish between the two prostatic diseases. This is further supported by the quantitative proteomic analysis utilizing ^{18}O isotope labeling where PSA peptides were identified with approximately equivalent expression levels in each tissue based on the observed $^{16}\text{O}/^{18}\text{O}$ isotope ratio (Fig. 5).

In the case of MIC-1, while four peptides were identified in the PCa-microdissected tissue extracts, no peptides were identified in the BPH-microdissected tissue extract, suggesting it is more abundant in PCa cells than BPH. Indeed, lack of MIC-1 protein expression has been associated with BPH (39), whereas high levels of MIC-1 expression have been linked to early prostate carcinogenesis (40). This result is further corroborated by the quantitative proteomic analysis where MIC-1 expression was detected in the cancer extract by isotopic labeling, whereas no MIC-1 expression was observed in the BPH extract, suggesting absence of expression in this case of BPH. In addition, a further 68 proteins were identified as differentially expressed between PCa and BPH by isotopic-labeling analysis.

FFPE tissues are a largely unexplored archive in MS-based proteomics. Therefore, it is important to understand the effects of formalin fixation and long-term storage on the samples. Unfortunately it is extremely difficult to identify unpredictable modifications within a complex mixture. Our results, however, show that just over 6% of the identified peptides contained a formylated lysine residue, and the percentage of oxidized methionine residues or peptides containing missed tryptic cleavages is not significantly different than that observed in proteomic studies of fresh cells (24, 26). Because we do not presently understand all of the possible modifications that may be observed in proteins extracted from FFPE tissues, biological information will primarily be obtained from the analysis of unmodified peptides.

The ability to conduct proteomic investigations of FFPE tissue has the potential to provide invaluable information regarding disease states and may aid in the development of improved clinical characterization and/or diagnostic techniques. Historically, the study of FFPE tissues has been limited to analysis of protein and RNA expression through use of affinity reagents such as antibodies or RNA probes (IHC and *in situ* hybridization). The methodology described here enables large scale proteomic technologies, such as MS, to be applied to vast archives of clinical and research tissues that had been previously thought of as intractable to such analyses. Use of tissue microdissection provides the ability to accurately correlate protein expression to histological infor-

mation for further investigation of a variety of proteins and their involvement in disease. In contrast to existing tissue microdissection approaches, the novel microdissection technology described here has been developed and optimized for procurement of cells directly from standard formalin-fixed tissue sections for downstream protein analysis. In addition, this technology is a noncontact method that explodes cells directly downward into a collection tube providing the added benefit of CAD/CAM automation for high throughput tissue microdissection capabilities.

The accurate diagnosis of prostate cancer is extremely challenging using current methodologies, and it is likely to benefit from using a panel of biomarkers. Indeed, the assessment of MIC-1 protein expression in conjunction with PSA testing may allow for distinction between BPH and frank PCa, alleviating incorrect diagnoses and further unnecessary tests.

* This work was supported by federal funds from the National Cancer Institute, National Institutes of Health, under contract NO1-CO-12400. The costs of publication of this article were defrayed in part by the payment of page charges. This article must therefore be hereby marked "advertisement" in accordance with 18 U.S.C. Section 1734 solely to indicate this fact.

§ The on-line version of this article (available at <http://www.mcponline.org>) contains supplemental material.

** To whom correspondence may be addressed: Laboratory of Proteomics and Analytical Technologies, National Cancer Institute, SAIC-Frederick, Inc., P.O. Box B, Frederick, MD 21702. Tel.: 301-846-7286; Fax: 301-846-6037; E-mail: veenstra@ncifcrf.gov.

‡‡ To whom correspondence may be addressed: Expression Pathology Inc., 9290 Gaither Rd., Gaithersburg, MD 20877. Tel.: 301-977-3654; Fax: 301-926-9283; E-mail: d.krizman@expressionpathology.com.

REFERENCES

- Schena, M., Shalon, D., Davis, R. W., and Brown, P. O. (1995) Quantitative monitoring of gene expression patterns with a complementary DNA microarray. *Science* **270**, 467–470
- DeRisi, J., Penland, L., Brown, P. O., Bittner, M. L., Meltzer, P. S., Ray, M., Chen, Y., Su, Y. A., and Trent, J. M. (1996) Use of a cDNA microarray to analyse gene expression patterns in human cancer. *Nat. Genet.* **14**, 457–460
- Krizman, D. B., Chuaqui, R. F., Meltzer, P. S., Trent, J. M., Duray, P. H., Linehan, W. M., Liotta, L. A., and Emmert-Buck, M. R. (1996) Construction of a representative cDNA library from prostatic intraepithelial neoplasia. *Cancer Res.* **56**, 5380–5383
- Strausberg, R. L., Greenhut, S. F., Grouse, L. H., Schaefer, C. F., and Buetow, K. H. (2001) *In silico* analysis of cancer through the Cancer Genome Anatomy Project. *Trends Cell Biol.* **11**, S66–S71
- Wasinger, V. C., and Corthals, G. L. (2002) Proteomic tools for biomedicine. *J. Chromatogr. B Analyt. Technol. Biomed. Life Sci.* **771**, 33–48
- MacIntyre, N. (2001) Unmasking antigens for immunohistochemistry. *Br. J. Biomed. Sci.* **58**, 190–196
- Shi, S. R., Cote, R. J., and Taylor, C. R. (2001) Antigen retrieval techniques: Current perspectives. *J. Histochem. Cytochem.* **49**, 931–937
- Ikeda, K., Monden, T., Kanoh, T., Tsujie, M., Izawa, H., Haba, A., Ohnishi, T., Sekimoto, M., Tomita, N., Shiozaki, H., and Monden, M. (1998) Extraction and analysis of diagnostically useful proteins from formalin-fixed, paraffin-embedded tissue sections. *J. Histochem. Cytochem.* **46**, 397–403
- Brooks, S. A., Dwek, M. V., and Leatham, A. J. (1998) Release and analysis of polypeptides and glycopolypeptides from formalin-fixed, paraffin wax-embedded tissue. *Histochem. J.* **30**, 609–615
- Izawa, H., Yamamoto, H., Ikeda, M., Fukunaga, H., Yasui, M., Ikenaga, M.,

- Sekimoto, M., Monden, T., Matsuura, N., and Monden, M. (2002) Analysis of cyclin D1 and CDK expression in colonic polyps containing neoplastic foci: A study of proteins extracted from paraffin sections. *Oncol. Rep.* **9**, 1313–1318
11. Emmert-Buck, M. R., Bonner, R. F., Smith, P. D., Chuaqui, R. F., Zhuang, Z., Goldstein, S. R., Weiss, R. A., and Liotta, L. A. (1996) Laser capture microdissection. *Science* **274**, 998–1001
 12. Gillespie, J. W., Ahram, M., Best, C. J., Swalwell, J. I., Krizman, D. B., Petricoin, E. F., Liotta, L. A., and Emmert-Buck, M. R. (2001) The role of tissue microdissection in cancer research. *Cancer J.* **7**, 32–39
 13. Knezevic, V., Leethanakul, C., Bichsel, V. E., Worth, J. M., Prabhu, V. V., Gutkind, J. S., Liotta, L. A., Munson, P. J., Petricoin, E. F., III, and Krizman, D. B. (2001) Proteomic profiling of the cancer microenvironment by antibody arrays. *Proteomics* **1**, 1271–1278
 14. Cohen, C. D., Grone, H. J., Grone, E. F., Nelson, P. J., Schlondorff, D., and Kretzler, M. (2002) c-myc antisense oligonucleotide treatment ameliorates murine ARPKD. *Kidney Int.* **61**, 125–132
 15. Gjerdrum, L. M., Sorensen, B. S., Kjeldsen, E., Sorensen, F. B., Nexø, E., and Hamilton-Dutoit, S. (2004) Real-time quantitative PCR of microdissected paraffin-embedded breast carcinoma: An alternative method for HER-2/neu analysis. *J. Mol. Diagn.* **6**, 42–51
 16. Gillespie, J. W., Best, C. J., Bichsel, V. E., Cole, K. A., Greenhut, S. F., Hewitt, S. M., Ahram, M., Gathright, Y. B., Merino, M. J., Strausberg, R. L., Epstein, J. I., Hamilton, S. R., Gannot, G., Baibakova, G. V., Calvert, V. S., Flaig, M. J., Chuaqui, R. F., Herring, J. C., Pfeifer, J., Petricoin, E. F., Linehan, W. M., Duray, P. H., Bova, G. S., and Emmert-Buck, M. R. (2002) Evaluation of non-formalin tissue fixation for molecular profiling studies. *Am. J. Pathol.* **160**, 449–457
 17. Ahram, M., Flaig, M. J., Gillespie, J. W., Duray, P. H., Linehan, W. M., Ornstein, D. K., Niu, S., Zhao, Y., Petricoin, E. F., III, and Emmert-Buck, M. R. (2003) Evaluation of ethanol-fixed, paraffin-embedded tissues for proteomic applications. *Proteomics* **3**, 413–421
 18. Sickmann, A., Mreyen, M., and Meyer, H. E. (2003) Mass spectrometry—A key technology in proteome research. *Adv. Biochem. Eng. Biotechnol.* **83**, 141–176
 19. Bodnar, W. M., Blackburn, R. K., Krise, J. M., and Moseley, M. A. (2003) Exploiting the complementary nature of LC/MALDI/MS/MS and LC/ESI/MS/MS for increased proteome coverage. *J. Am. Soc. Mass Spectrom.* **14**, 971–979
 20. Chaurand, P., Schwartz, S. A., and Caprioli, R. M. (2004) Assessing protein patterns in disease using imaging mass spectrometry. *J. Proteome Res.* **3**, 245–252
 21. Peng, J., and Gygi, S. P. (2001) Proteomics: The move to mixtures. *J. Mass Spectrom.* **36**, 1083–1091
 22. Zang, L., Palmer Toy, D., Hancock, W. S., Sgroi, D. C., and Karger, B. L. (2004) Proteomic analysis of ductal carcinoma of the breast using laser capture microdissection, LC-MS, and $^{16}\text{O}/^{18}\text{O}$ isotopic labeling. *J. Proteome Res.* **3**, 604–612
 23. Baker, H., Patel, V., Molinob, A. A., Shillitoe, E. J., Ensley, J. F., Yoo, G. H., Meneses-Garcia, A., Myers, J. N., El-Naggar, A. K., Gutkind, J. S., and Hancock, W. S. (2005) Proteome-wide analysis of head and neck squamous cell carcinomas using laser-capture microdissection and tandem mass spectrometry. *Oral Oncol.* **41**, 183–199
 24. Peng, J., Elias, J. E., Thoreen, C. C., Licklider, L. J., and Gygi, S. P. (2003) Evaluation of multidimensional chromatography coupled with tandem mass spectrometry (LC/LC-MS/MS) for large-scale protein analysis: The yeast proteome. *J. Proteome Res.* **2**, 43–50
 25. Kyte, J., and Doolittle, R. F. (1982) A simple method for displaying the hydropathic character of a protein. *J. Mol. Biol.* **157**, 105–132
 26. Yu, L. R., Conrads, T. P., Uo, T., Kinoshita, Y., Morrison, R. S., Lucas, D. A., Chan, K. C., Blonder, J., Issaq, H. J., and Veenstra, T. D. (2004) Global analysis of the cortical neuron proteome. *Mol. Cell Proteomics* **3**, 896–907
 27. Hood, B. L., Lucas, D. A., Kim, G., Chan, K. C., Blonder, J., Issaq, H. J., Veenstra, T. D., Conrads, T. P., Pollet, I., and Karsan, A. (2005) Quantitative analysis of the low molecular weight serum proteome using ^{18}O stable isotope labeling in a lung tumor xenograft mouse model. *J. Am. Soc. Mass Spectrom.* **16**, 1221–1230
 28. Yao, X., Freas, A., Ramirez, J., Demirev, P. A., and Fenselau, C. (2001) Proteolytic ^{18}O labeling for comparative proteomics: model studies with two serotypes of adenovirus. *Anal. Chem.* **73**, 2836–2842
 29. Schnolzer, M., Jedrzejewski, P., and Lehmann, W. D. (1996) Protease-catalyzed incorporation of ^{18}O into peptide fragments and its application for protein sequencing by electrospray and matrix-assisted laser desorption/ionization mass spectrometry. *Electrophoresis* **17**, 945–953
 30. Rose, K., Simona, M. G., Offord, R. E., Prior, C. P., Otto, B., and Thatcher, D. R. (1983) A new mass spectrometric C-terminal sequencing technique finds a similarity between γ -interferon and $\alpha 2$ -interferon and identifies a proteolytically clipped γ -interferon that retains full antiviral activity. *Biochem. J.* **215**, 273–277
 31. Lin, M. F., DaVolio, J., and Garcia-Arenas, R. (1992) Expression of human prostatic acid phosphatase activity and the growth of prostate carcinoma cells. *Cancer Res.* **52**, 4600–4607
 32. Stamey, T. A., Yang, N., Hay, A. R., McNeal, J. E., Freiha, F. S., and Redwine, E. (1987) Prostate-specific antigen as a serum marker for adenocarcinoma of the prostate. *N. Engl. J. Med.* **317**, 909–916
 33. Lowe, F. C., and Trauzzi, S. J. (1993) Prostatic acid phosphatase in 1993. Its limited clinical utility. *Urol. Clin. North Am.* **20**, 589–595
 34. Bottner, M., Suter-Crazzolara, C., Schober, A., and Unsicker, K. (1999) Expression of a novel member of the TGF- β superfamily, growth/differentiation factor-15/macrophage-inhibiting cytokine-1. *Cell Tissue Res.* **297**, 103–110
 35. Yang, H., Filipovic, Z., Brown, D., Breit, S. N., and Vassilev, L. T. (2003) Macrophage inhibitory cytokine-1: A novel biomarker for p53 pathway activation. *Mol. Cancer Ther.* **2**, 1023–1029
 36. Lindmark, F., Zheng, S. L., Wiklund, F., Bensen, J., Balter, K. A., Chang, B., Hedelin, M., Clark, J., Stattin, P., Meyers, D. A., Adami, H. O., Isaacs, W., Gronberg, H., and Xu, J. (2004) H6D polymorphism in macrophage-inhibitory cytokine-1 gene associated with prostate cancer. *J. Natl. Cancer Inst.* **96**, 1248–1254
 37. Keller, E. T., Fu, Z., and Brennan, M. (2004) The role of Raf kinase inhibitor protein (RKIP) in health and disease. *Biochem. Pharmacol.* **68**, 1049–1053
 38. Keller, E. T., Fu, Z., and Brennan, M. (2005) The biology of a prostate cancer metastasis suppressor protein: Raf kinase inhibitor protein. *J. Cell Biochem.* **94**, 273–278
 39. Kakehi, Y., Segawa, T., Wu, X. X., Kulkarni, P., Dhir, R., and Getzenberg, R. H. (2004) Down-regulation of macrophage inhibitory cytokine-1/prostate derived factor in benign prostatic hyperplasia. *Prostate* **59**, 351–356
 40. Cheung, P. K., Woolcock, B., Adomat, H., Sutcliffe, M., Bainbridge, T. C., Jones, E. C., Webber, D., Kinahan, T., Sadar, M., Gleave, M. E., and Vielkind, J. (2004) Protein profiling of microdissected prostate tissue links growth differentiation factor 15 to prostate carcinogenesis. *Cancer Res.* **64**, 5929–5933